

Evolution of Fock states in three mixed harmonic oscillators: quantum statistics

Faisal A. A. El-Orany*, J. Peřina¹ and M. Sebawe Abdalla²

¹ *Joint Laboratory of Optics of Palacký University and
Physical Institute of Academy of Sciences of Czech Republic,
17. listopadu 50, 772 07 Olomouc, Czech Republic.*

² *Mathematics Department, College of Science,
King Saud University, P.O. Box 2455, Riyadh 11451, Saudi Arabia*

In this communication we investigate the quantum statistics of three harmonic oscillators mutually interacting with each other considering the modes are initially in Fock states. After solving the equations of motion, the squeezing phenomenon, sub-Poissonian statistics and quasiprobability functions are discussed. We demonstrate that the interaction is able to produce squeezing of different types. We show also that certain types of Fock states can evolve in this interaction into thermal state and squeezed thermal state governed by the interaction parameters.

PACS numbers: 42.50Dv, 42.60.Gd

Key words: Quasiprobability functions; nonlinear coupler; squeezed light; quantum phase

I. INTRODUCTION

In the field of nonlinear optics there are two basic parametric processes, namely, parametric amplifier and frequency converter. The parametric amplifier is designed to amplify an oscillating signal by means of a particular coupling of the mode to the second mode of oscillation, the idler mode. The coupling parameter is made to oscillate with time in a way which gives rise to a steady increase of the energy in both the signal and idler modes [1]. The parametric amplifier is the source of squeezed light (i.e. the states of light with reduced

* Permanent address: Suez Canal university, Faculty of Science, Department of mathematics and computer science, Ismailia, Egypt.

fluctuations in one quadrature below the level associated with the vacuum state [2]). To be more specific the degenerate and non-degenerate parametric amplifier are the sources for single-mode and two-mode squeezing, respectively. The lossless Hamiltonian describing such a system (non-degenerate case) is given by

$$\frac{\hat{H}}{\hbar} = \sum_{j=1}^2 \omega_j \hat{a}_j^\dagger \hat{a}_j + i\lambda_1 \{ \hat{a}_1 \hat{a}_2 \exp[i(\omega_1 + \omega_2)t] - \text{h.c.} \}, \quad (1.1)$$

where \hat{a}_j^\dagger and \hat{a}_j are the creation and annihilation operators, λ_1 is the coupling constant including the amplitude of the pump, and $\omega_j, j = 1, 2$ are the field frequencies. On the other hand, the parametric frequency converter is described by a process of exchanging photons between two optical fields of different frequencies. The Hamiltonian representing such a system reads

$$\frac{\hat{H}}{\hbar} = \sum_{j=1}^2 \omega_j \hat{a}_j^\dagger \hat{a}_j + i\lambda_2 \{ \hat{a}_1^\dagger \hat{a}_2 \exp[i(\omega_1 - \omega_2)t] - \text{h.c.} \}. \quad (1.2)$$

This model can be applied to describe various optical phenomena, e.g. to find analogies between frequency converter and beam splitter [3], two-level atom driven by a single mode of electromagnetic field [4], and Raman scattering [3, 5]. The quantum properties of parametric frequency converter are discussed in [6]. Furthermore, some authors studied this model as the lossless linear coupler, e.g. in [7]. In this situation the model is considered to be represented by two electromagnetic waves which are guided inside the structure consisting of two adjacent and parallel waveguides; the linear exchange of energy between these two waveguides is established via the evanescent field [8].

The derivation of the above Hamiltonians can be obtained from the quantization of the cavity modes in a volume V . In this case the total energy of the field is given by [6, 9]

$$\hat{H} = \frac{1}{8\pi} \int_{cavity} (\epsilon \mathcal{E}^2 + \mathcal{H}^2) d^3V, \quad (1.3a)$$

where \mathcal{E} and \mathcal{H} are the electric and magnetic fields, respectively, and ϵ is the dielectric constant. To provide coupling between the various cavity modes we have to make the dielectric constant ϵ varied according to

$$\epsilon(R, t) = 1 + \Delta \epsilon f(R) \sum_i \cos(\omega_i t + \phi_i), \quad (1.3b)$$

where $\Delta\epsilon \ll 1$ and $f(R)$ is a function of the position vector R , while ϕ_i is an arbitrary pump phase. From the relations (1.3a) and (1.3b), and in terms of the boson operators, one can write the Hamiltonian (1.3a) in the following form

$$\frac{\hat{H}}{\hbar} = \sum_l \omega_l (\hat{a}_l^\dagger \hat{a}_l + \frac{1}{2}) - \sum_{i,l,m} k_{lm} \cos(\omega_i t + \phi_i) (\hat{a}_l^\dagger - \hat{a}_l) (\hat{a}_m^\dagger - \hat{a}_m), \quad (1.3c)$$

where k_{lm} is the coupling coefficient having the form

$$k_{lm} = \frac{\Delta\epsilon}{16\pi c^2} (\omega_l \omega_m)^{\frac{1}{2}} \int_{cavity} f(r) u_l(r) u_m(r) dV, \quad (1.3d)$$

where the function $u_l(r)$ represents the normal mode and satisfies

$$\nabla \wedge \nabla \wedge u_l(r) = \left(\frac{\omega_l}{c}\right)^2 u_l(r). \quad (1.3e)$$

It is convenient to refer to the recent work of Garrett et al. [10], who reported an experimental demonstration of phonon squeezing in a macroscopic system by exciting a crystal KTaO_3 with an ultrafast pulse of light. The Hamiltonian relevant to their work can be adjusted to be essentially equation (1.3c). Thus if one chooses the function $f(R)$ so that $k_{lm} \neq 0$, this will leave an infinite number of modes coupled. Hence by a proper choice of the pump frequency ω_i , the interacting modes will be limited to two modes, and then under certain conditions one can obtain the Hamiltonians (1.1) or (1.2).

The optical processes involving the competition between frequency converter and parametric amplifier are of interest from theoretical and experimental points of view, which can be seen in three-mode interaction [11, 12] and nonlinear coupler [13, 14], where the nonlinear interaction couples different photon modes and leads to the energy transfer between modes. Photons in some modes may be annihilated, while those in the other modes created, and hence the photon distribution is disturbed. In each time the rate of energy transfer between the modes depends on the statistical properties of the light fields. This in fact encouraged us to follow up the procedure given above and adjust the pump frequency to extend the number of modes to be three instead of two. This can lead to the following Hamiltonian

$$\begin{aligned} \frac{\hat{H}}{\hbar} = & \left[\sum_{j=1}^3 \omega_j \hat{a}_j^\dagger \hat{a}_j \right] + i\lambda_1 \{ \hat{a}_1 \hat{a}_2 \exp[i(\omega_1 + \omega_2)t] - \text{h.c.} \} \\ & + i\lambda_2 \{ \hat{a}_1 \hat{a}_3^\dagger \exp[i(\omega_1 - \omega_3)t] - \text{h.c.} \} + i\lambda_3 \{ \hat{a}_2 \hat{a}_3^\dagger \exp[i(\omega_2 - \omega_3)t] - \text{h.c.} \}, \end{aligned} \quad (1.4)$$

which represents a model of three boson field modes, designated by the annihilation operators $\hat{a}_j, j = 1, 2, 3$, and an intense monochromatic light wave inducing parametric coupling between them. In this Hamiltonian λ_j are the coupling constants including the pump amplitude and proportional to the second-order susceptibility of the medium $\chi^{(2)}$; ω_j are the natural frequencies of oscillation of the uncoupled modes and h.c. is the Hermitian conjugate. This interaction can also be established, e.g. by means of a bulk nonlinear crystal exhibiting the second-order nonlinear properties in which three dynamical modes of frequencies $\omega_1, \omega_2, \omega_3$ are induced by three beams from lasers of these frequencies. When pumping this crystal by means of the corresponding strong coherent pump beams, as indicated in the Hamiltonian, we can approximately fulfil the phase-matching conditions for the corre-

sponding processes, in particular if the frequencies are close each other (biaxial crystals may be helpful in such an arrangement). Also a possible use of quasi-phase matching may help in the realization, which is, however, more difficult technologically [15]. There is another possibility to realize the interaction described by the Hamiltonian (1.4) using a nonlinear asymmetric directional coupler as shown schematically in Fig. 1.

For completeness, Hamiltonian (1.4) is a generalization for several models used in the literature, e.g. [1, 11, 16], and it is invariant under the transformation $\hat{a}_1 \longleftrightarrow \hat{a}_2$ with $\lambda_2 \longleftrightarrow \lambda_3$. So that the equations of the 2nd mode can be obtained from those of the first one.

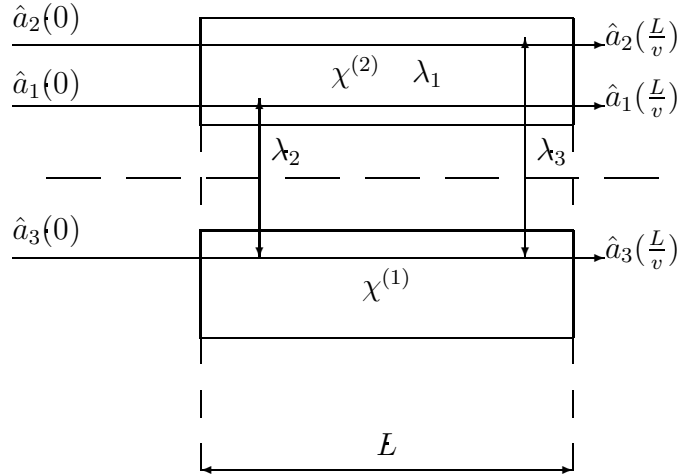


Fig.1 Scheme of realization of interaction in (1.4) using a nonlinear asymmetric directional coupler which is composed of two optical waveguides fabricated from first-order ($\chi^{(1)}$) and second-order ($\chi^{(2)}$) materials, where χ designate susceptibility. Modes 1 and 2 propagate in the first waveguide and mode 3 in the second waveguide. The interaction between modes 1 and 2 is established by strong pump coherent light, which is not indicated in figure, with the coupling constant λ_1 . The interactions between mode 3 and modes 1 and 2 are established linearly with the coupling constants λ_2 and λ_3 , respectively. The beams are described by the photon annihilation operators as indicated; $z = vt$ is the interaction length and we assume that all beams have the same velocity v and the length of the waveguides is L . Outgoing fields are examined as single or compound modes by means of homodyne detection to observe squeezing of vacuum fluctuations, or by means of a set of photodetectors to measure photon correlations, photon antibunching and sub-Poissonian photon statistics in the standard ways.

In this article we investigate the statistical properties for the different modes controlled by the Hamiltonian (1.4). We consider the modes are initially prepared in Fock (number) states where these states represent the most basic quantum states and are maximally distant from what one would call a classical field. More illustratively, they can always exhibit sub-Poissonian statistics, however, they provide no information on the phase since the number of photons is quite certain. Also any states can be expressed in terms of these states with corresponding weighting distributions. Further, there are various proposals how to generate such states. For instance, these states can be prepared in a nondemolition measurements [17–19] or in the micromaser [20]. During this work we use a finite number of quanta in each modes, which is relevant to the experimental realization. Also we treat the model as three harmonic oscillators interacting in a nonlinear crystal in a sense of a competition between two frequency converters and one parametric amplifier, as indicated in the Hamiltonian (1.4). Under these circumstances the model is motivated by various interesting results. For example, we show that this model can be used as an effective source for squeezed light additionally to those systems given in the literature earlier [21]. Also we show that it can yield thermal light and squeezed thermal light. Moreover, we demonstrate how the qualitative behaviour of the single nonlinear process such as parametric amplifier or frequency converter can be substantially changed in the presence of the other nonlinear processes.

The plan of the work is as follows: In **section 2** we introduce the solution of the equations of motion, **section 3** is devoted to a discussion of nonclassical phenomena such as quadrature squeezing, second-order correlation function and the violation of Cauchy-Schwarz inequality, in **section 4** we demonstrate the quasidistribution functions, and finally we summarize main conclusions in **section 5**.

II. SOLUTION OF THE EQUATIONS OF MOTION

In this section we shall introduce the exact solution for the equations of motion in the Heisenberg picture for the Hamiltonian (1.4).

The dynamics of the system is described by the Heisenberg equations of motion which for any operator \hat{O} are given by

$$\frac{d\hat{O}}{dt} = \frac{\partial\hat{O}}{\partial t} + \frac{1}{i\hbar}[\hat{O}, \hat{H}], \quad (2.1)$$

where [...,...] represents the commutator.

Therefore the propagation of the field operators, which are defined in the slowly varying forms ($\hat{a}_j = \hat{A}_j \exp(-i\omega_j t)$, $j = 1, 2, 3$), can be written in the following form:

$$\frac{d\hat{A}_1}{dt} = -\lambda_1 \hat{A}_2^\dagger - \lambda_2 \hat{A}_3, \quad (2.2a)$$

$$\frac{d\hat{A}_2}{dt} = -\lambda_1 \hat{A}_1^\dagger - \lambda_3 \hat{A}_3, \quad (2.2b)$$

$$\frac{d\hat{A}_3}{dt} = \lambda_2 \hat{A}_1 + \lambda_3 \hat{A}_2. \quad (2.2c)$$

These are three equations with their Hermitian conjugates forming a closed system which can be solved easily as

$$\begin{aligned} \hat{A}_1(t) &= \hat{a}_1(0)f_1(t) + \hat{a}_1^\dagger(0)f_2(t) - \hat{a}_2(0)f_3(t) \\ &\quad - \hat{a}_2^\dagger(0)f_4(t) - \hat{a}_3(0)f_5(t) - \hat{a}_3^\dagger(0)f_6(t), \end{aligned} \quad (2.3a)$$

$$\begin{aligned} \hat{A}_2(t) &= \hat{a}_2(0)g_1(t) + \hat{a}_2^\dagger(0)g_2(t) - \hat{a}_1(0)g_3(t) \\ &\quad - \hat{a}_1^\dagger(0)g_4(t) - \hat{a}_3(0)g_5(t) - \hat{a}_3^\dagger(0)g_6(t), \end{aligned} \quad (2.3b)$$

$$\begin{aligned} \hat{A}_3(t) &= \hat{a}_3(0)h_1(t) + \hat{a}_3^\dagger(0)h_2(t) + \hat{a}_2(0)h_3(t) \\ &\quad + \hat{a}_2^\dagger(0)h_4(t) + \hat{a}_1(0)h_5(t) + \hat{a}_1^\dagger(0)h_6(t), \end{aligned} \quad (2.3c)$$

where the exact forms for the time-dependent coefficients, i.e. for $f_j(t), g_j(t), h_j(t)$, which include all information about the structure of the model are complicated for the general case, we give their form only for the special case when $\lambda_2 = \lambda_3 = \lambda$ (hence $f_j(t) = g_j(t)$), which will be frequently used here:

$$\begin{aligned} f_{1,3}(t) &= \pm \frac{1}{2} \left[\cosh\left(\frac{\lambda_1 t}{2}\right) \cos(\bar{k}t) + \frac{\lambda_1}{2k} \sinh\left(\frac{\lambda_1 t}{2}\right) \sin(\bar{k}t) \pm \cosh(\lambda_1 t) \right], \\ f_{2,4}(t) &= \mp \frac{1}{2} \left[\sinh\left(\frac{\lambda_1 t}{2}\right) \cos(\bar{k}t) + \frac{\lambda_1}{2k} \cosh\left(\frac{\lambda_1 t}{2}\right) \sin(\bar{k}t) \mp \sinh(\lambda_1 t) \right], \\ f_5(t) &= \frac{\lambda}{\bar{k}} \cosh\left(\frac{\lambda_1 t}{2}\right) \sin(\bar{k}t), \quad f_6(t) = -\frac{\lambda}{\bar{k}} \sinh\left(\frac{\lambda_1 t}{2}\right) \sin(\bar{k}t), \end{aligned} \quad (2.4)$$

$$\begin{aligned} h_1(t) &= \cosh\left(\frac{\lambda_1 t}{2}\right) \cos(\bar{k}t) - \frac{\lambda_1}{2k} \sinh\left(\frac{\lambda_1 t}{2}\right) \sin(\bar{k}t), \\ h_2(t) &= -\sinh\left(\frac{\lambda_1 t}{2}\right) \cos(\bar{k}t) + \frac{\lambda_1}{2k} \cosh\left(\frac{\lambda_1 t}{2}\right) \sin(\bar{k}t), \\ h_3(t) &= h_5(t) = \frac{\lambda}{\bar{k}} \cosh\left(\frac{\lambda_1 t}{2}\right) \sin(\bar{k}t), \quad h_4(t) = h_6(t) = -\frac{\lambda}{\bar{k}} \sinh\left(\frac{\lambda_1 t}{2}\right) \sin(\bar{k}t), \end{aligned} \quad (2.5)$$

where $\bar{k} = \sqrt{2\lambda^2 - \frac{\lambda_1^2}{4}}$. In fact, the nature of the solution can show how the interaction does work. That is the time-dependent coefficients contain both trigonometric and hyperbolic functions. Consequently, the energy associated with the propagating beams inside the

nonlinear crystal can be amplified as well as switched between modes in the course of time.

On the basis of the well known commutation rules for boson operators, the following relations can be proved between the time-dependent coefficients

$$\begin{aligned} f_1^2(t) - f_2^2(t) + f_3^2(t) - f_4^2(t) + f_5^2(t) - f_6^2(t) &= 1, \\ f_1(t)g_4(t) - f_2(t)g_3(t) + f_3(t)g_2(t) - f_4(t)g_1(t) - f_5(t)g_6(t) + f_6(t)g_5(t) &= 0, \\ f_1(t)g_3(t) - f_2(t)g_4(t) + f_3(t)g_1(t) - f_4(t)g_2(t) - f_5(t)g_5(t) + f_6(t)g_6(t) &= 0. \end{aligned} \quad (2.6)$$

The remain relations can be obtained from (2.6) by means of the following transformations

$$\begin{aligned} &\left(f_1(t), f_2(t), f_3(t), f_4(t), f_5(t), f_6(t) \right) \\ &\longleftrightarrow \left(-g_3(t), -g_4(t), -g_1(t), -g_2(t), g_5(t), g_6(t) \right) \\ &\longleftrightarrow \left(h_5(t), h_6(t), -h_3(t), -h_4(t), -h_1(t), -h_2(t) \right). \end{aligned} \quad (2.7)$$

Based on the results of the present section, we can study the quantum properties of the evolution of the different modes in the model when they are initially prepared in Fock states.

III. NONCLASSICAL PHENOMENA

Since the photons produced in a nonlinear optical process are known to possess unusual correlation properties resulting in many of nonclassical aspects of the radiation field. Therefore, we investigate some of these properties for the model under consideration in the present section. Our attention is focused on squeezing phenomenon, sub-Poissonian photon statistics and the violation of Cauchy-Schwarz inequality.

A. Squeezing phenomenon

The concept of squeezing of a quantum electromagnetic field has been given a great deal of interest in the view of the possibility of reducing the noise of an optical signal below the vacuum limit and the possible potential application in optical communication networks [2] and gravitational wave detection [22]. This light can be measured by homodyne detection where the signal is superimposed on a strong coherent beam of the local oscillator. The generation of such light has been reported in various schemes [23].

Generally there are several definitions for squeezing, e.g. see [21]. Here we investigate some of these types for the model under discussion, in particular, single-mode, two-mode and three-mode squeezing as well as sum-squeezing [24] when the modes are prepared initially in

Fock states. The starting point for this study are the two quadratures \hat{X} and \hat{Y} which are related to the conjugate electric and magnetic field operators \hat{E} and \hat{H} . They are defined in the standard way. Assuming that these two quadrature operators satisfy the following commutation relation

$$[\hat{X}, \hat{Y}] = \hat{C}, \quad (3.1a)$$

where \hat{C} may be an operator or a c-number with respect to which kind of squeezing we consider, the following uncertainty relation holds

$$\langle (\Delta \hat{X})^2 \rangle \langle (\Delta \hat{Y})^2 \rangle \geq \frac{|\langle \hat{C} \rangle|^2}{4}, \quad (3.1b)$$

where $\langle (\Delta \hat{X})^2 \rangle = \langle \hat{X}^2 \rangle - \langle \hat{X} \rangle^2$ is the variance. Therefore, we can say that the model possesses X -quadrature squeezing if the S -factor [25],

$$S(t) = \frac{\langle (\Delta \hat{X}(t))^2 \rangle - 0.5|\langle \hat{C} \rangle|}{0.5|\langle \hat{C} \rangle|}, \quad (3.1c)$$

satisfies the inequality $-1 \leq S < 0$. Similar expression for the Y -quadrature (Q -factor) can be obtained.

Firstly, for three-mode squeezing we define the two quadratures as

$$\hat{X}_3(t) = \frac{1}{2}[\hat{A}_1(t) + \hat{A}_2(t) + \hat{A}_3(t) + \hat{A}_1^\dagger(t) + \hat{A}_2^\dagger(t) + \hat{A}_3^\dagger(t)], \quad (3.2a)$$

$$\hat{Y}_3(t) = \frac{1}{2i}[\hat{A}_1(t) + \hat{A}_2(t) + \hat{A}_3(t) - \hat{A}_1^\dagger(t) - \hat{A}_2^\dagger(t) - \hat{A}_3^\dagger(t)], \quad (3.2b)$$

where the subscript 3 in the left-hand side stands for three mode case. Using (2.3) together with the definition of the variance, for initial Fock states we arrive at

$$\begin{aligned} 4\langle (\Delta \hat{X}_3(t))^2 \rangle &= (1 + 2\bar{n}_1)[f_1(t) + f_2(t) + h_5(t) + h_6(t) - g_3(t) - g_4(t)]^2 \\ &+ (1 + 2\bar{n}_2)[f_3(t) + f_4(t) - g_1(t) - g_2(t) - h_3(t) - h_4(t)]^2 \\ &+ (1 + 2\bar{n}_3)[f_5(t) + f_6(t) + g_5(t) + g_6(t) - h_1(t) - h_2(t)]^2, \end{aligned} \quad (3.3a)$$

$$\begin{aligned} 4\langle (\Delta \hat{Y}_3(t))^2 \rangle &= (1 + 2\bar{n}_1)[f_1(t) + g_4(t) + h_5(t) - f_2(t) - g_3(t) - h_6(t)]^2 \\ &+ (1 + 2\bar{n}_2)[f_3(t) + g_2(t) + h_4(t) - f_4(t) - g_1(t) - h_3(t)]^2 \\ &+ (1 + 2\bar{n}_3)[f_5(t) + g_5(t) + h_2(t) - f_6(t) - g_6(t) - h_1(t)]^2; \end{aligned} \quad (3.3b)$$

\bar{n}_j is the mean photon number for the j th mode. The expressions for the single-mode and two-mode squeezing can be obtained easily from (3.3) for two quadratures defined in a manner analogous to (3.2) by dropping the coefficients of the absent mode, e.g. for the 1st mode, single-mode squeezing can be obtained by setting $g_j(t) = h_j(t) = 0, j = 1, 2, 3$ in (3.3). It should be taken into account that \hat{C} is a c-number in this case and equals $\frac{1}{2}, 1, \frac{3}{2}$ corresponding to the single-mode, two-mode and three-mode squeezing, respectively.

We start our discussion when $\lambda_2 = \lambda_3 = \lambda$. In this case the quadrature variances for the 3rd mode (single-mode squeezing) are

$$\langle (\Delta \hat{X}_1(t))^2 \rangle = \frac{1}{4} \left\{ 2(1 + \bar{n}_1 + \bar{n}_2) \left[\frac{\lambda}{\bar{k}} \sin(\bar{k}t) \right]^2 + (1 + 2\bar{n}_3) \left[\cos(\bar{k}t) + \frac{\lambda_1}{2\bar{k}} \sin(\bar{k}t) \right]^2 \right\} \exp(-\lambda_1 t), \quad (3.4a)$$

$$\langle (\Delta \hat{Y}_1(t))^2 \rangle = \frac{1}{4} \left\{ 2(1 + \bar{n}_1 + \bar{n}_2) \left[\frac{\lambda}{\bar{k}} \sin(\bar{k}t) \right]^2 + (1 + 2\bar{n}_3) \left[\cos(\bar{k}t) - \frac{\lambda_1}{2\bar{k}} \sin(\bar{k}t) \right]^2 \right\} \exp(\lambda_1 t). \quad (3.4b)$$

The immediate conclusion can be drawn from these expressions which is that there is squeezing in the X -quadrature after switching on of the interaction by a suitable time as a result of the fact that the Fock states are not minimum-uncertainty states. Indeed, this is an interesting result because most of the nonlinear optical processes including correlation of modes are unable to provide such a property. Furthermore, under this condition similar expressions, i.e. $(...) \exp(-\lambda_1 t)$ for X -quadrature and $(...) \exp(\lambda_1 t)$ for Y -quadrature, can be obtained for the two-mode squeezing, in particular, between the 1st and 2nd modes and also for the three-mode squeezing. Also, this situation is still valid if one considers that the modes are initially in the states which are represented by a density matrix diagonal in the number state basis (thermofield states); in this case \bar{n}_j represents the average photon number for the j th thermal mode and therefore the behaviour of the model under consideration is close to that of a microwave Josephson-junction parametric amplifier [26], in which a thermal input field has been introduced to the squeezing device and the generated field has exhibited noise reduction. Indeed, thermal noise is inevitable and hard to quench, so that it is more realistic to consider a thermal state instead of a vacuum state input to a squeezing device [27]. More details about the properties of squeezed number and squeezed thermal states can be found in [27, 28]. We proceed by plotting the squeezing factors associated with the X -quadrature, i.e. S -factor, for the three types when the modes are initially in the Fock states as shown in Fig. 2, for the given values of the parameters. In this figure we have considered the single-mode (star-centered curve-3rd mode), two-mode (short-dashed curve-(1,2) modes) and three-mode squeezing (long-dashed curve). For the sake of comparison we adopted solid curve for squeezing factor of well-known squeezed number states [29], i.e. for $S_1(t) = (1 + 2\bar{n}) \exp(-\lambda_1 t) - 1$, $r = \lambda_1 t$ is the usual squeeze parameter. From this figure we can see that for all cases at the first moments of the evolution there is no squeezing

owing to the nature of the Fock states. Further, the three types have approximately similar behaviours in a sense that they oscillate around the value of the usual squeezed number states, i.e. around the solid curve, as a result of switching of the energy between the interacting modes in the system. The significant remark is that they arrive to the steady state (maximum squeezing) at the large values of interaction times.

From the above analysis it is clear that the 3rd mode possesses more pronounced nonclassical behaviour compared with the 1st and 2nd modes. This is related to the structure of the Hamiltonian (1.4) and can be interpreted as follows: modes 1 and 2 undergo amplification from the first process (i.e. from the parametric amplifier) and then the energy transfers from these two modes to the 3rd mode via the converter processes. Indeed, such a structure is the source of the single-mode squeezing which has not been seen before for the most of the important models involving three-mode interaction process, e.g. [11, 30].

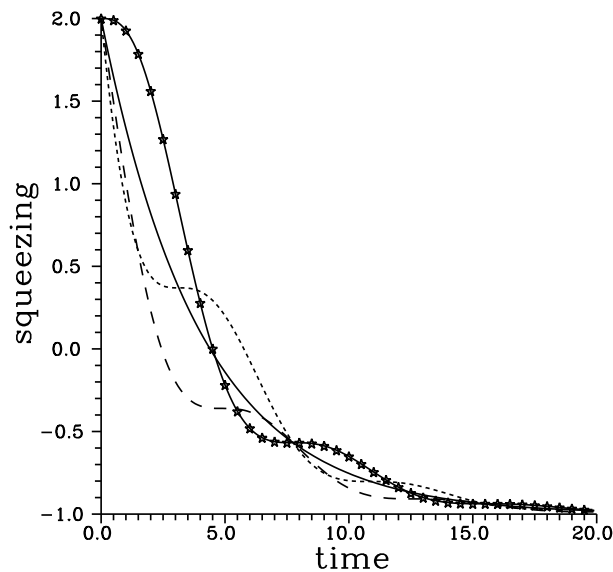


FIG. 2: Squeezing factor, $S_n(t)$, for initial number states with mean photon numbers $\bar{n}_j = 1$, $j = 1, 2, 3$, against the time for the single-mode (star-centered curve-3rd mode), two-mode (short-dashed curve-(1,2) modes) and three-mode squeezing (long-dashed curve) for $(\lambda_1, \lambda_2, \lambda_3) = (0.25, 0.3, 0.3)$; the solid curve is for squeezed number states, i.e. for $S_1(t) = (1+2n) \exp(-\lambda_1 t) - 1$, $\lambda_1 t$ represents the usual squeeze parameter r .

Secondly, we discuss sum-squeezing [24] for the model under discussion. Sum-squeezing effect is both higher-order and multimode phenomenon and the states join to this class are nonclassical states since its Glauber-Sudarshan P -function always does not exist and it is not

well defined function. Also, there is a connection between sum-squeezing and sum-frequency generation and consequently it can be converted into normal single-mode squeezing by an appropriate nonlinear optical process and this may be used for the detection. The importance of this type is related to the fact that squeezing can exist for the correlated modes even if the individual modes are not squeezed in the normal sense.

Now the quadratures corresponding to the real and imaginary parts for sum-squeezing are given by [24]

$$\hat{X}_s(t) = \frac{1}{2}[\hat{A}_j(t)\hat{A}_k(t) + \hat{A}_j^\dagger(t)\hat{A}_k^\dagger(t)], \quad (3.5a)$$

$$\hat{Y}_s(t) = \frac{1}{2i}[\hat{A}_j(t)\hat{A}_k(t) - \hat{A}_j^\dagger(t)\hat{A}_k^\dagger(t)], \quad (3.5b)$$

where $j \neq k$ and the subscript s stands for sum-squeezing. In this case $\hat{C} = \hat{A}_j^\dagger(t)\hat{A}_j(t) + \hat{A}_k^\dagger(t)\hat{A}_k(t) + 1$, i.e. it is a state dependent. One should notice that the amplitude squared squeezing [31] is the degenerate limit of sum-squeezing, and also the operators $\hat{X}_s(t), \hat{Y}_s(t), \hat{C}$ form a representation of the $su(1,1)$ Lie algebra and thus they have been used in the interferometric measurements [32].

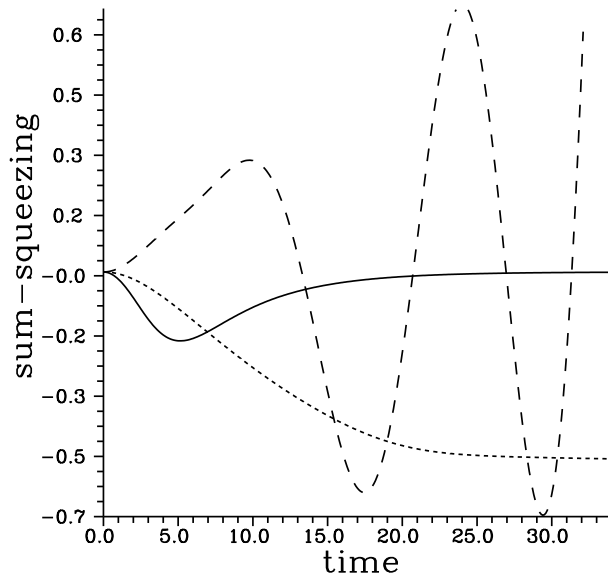


FIG. 3: Sum-squeezing factor for initial number states with mean photon numbers $\bar{n}_j = 1$, $j = 1, 2, 3$, against the time for $\lambda_j = 0.1, j = 1, 2, 3$ and for the single parametric amplifier (Y-component, solid curve), between modes 1,2 (Y-component, short-dashed curve) and between modes 1,3 (X-component, long-dashed curve).

The expressions for $S(t)$ and $Q(t)$ for sum-squeezing are rather lengthy in this case, further, they can be calculated straightforwardly and are not very illuminating, so we shall

not quote their explicit forms. As is known the single parametric amplifier is the source of sum-squeezed light [33], however, single frequency converter cannot produce such a light. The system under consideration can produce sum-squeezed light which is more effective than that of the single parametric amplifier and this reflects the role of competition of different processes in the model. These facts are clear in Fig. 3 where the sum-squeezing factor is plotted against the time for the shown values of the parameters. Solid, short-dashed and long-dashed curves show that sum-squeezing factor corresponds to the Y -component of single parametric amplifier, the Y -component of (1,2) compound mode and the X -component of (1,3) compound mode, respectively. From this figure one can observe that for the single parametric amplifier (solid curve), it starts from squeezing bound, goes to its maximum squeezing value ($\simeq 12\%$) and then squeezing values decrease and eventually comes back to the initial values for large interaction times. However, for (1,2) mode, squeezing appears after switching on of the interaction as before, then its value increases in the course of time and eventually locks to give 50% squeezing in the large time of interaction domain. It is important to point out neither the 1st mode nor the 2nd one is squeezed in the normal sense in this case. We proceed by discussing the quantity for (1,3) mode (long-dashed curve). One can observe that squeezing is periodically established displaying its maximum value in the large interaction time and then squeezing disappears (this is not indicated in the figure). The maximum value of the sum-squeezing in this case is more pronounced than in the previous ones, in particular, up to 70% squeezing can be obtained. We should remind here that the 3rd mode can produce squeezing in the normal sense (cf. (3.4)). Consequently we can conclude that there is no connection between sum-squeezing and normal squeezing for the models including correlation between modes [24]. It is important to point out that the behaviour of the sum-squeezing in (2,3) mode is similar to that for (1,3) mode and this can be recognized from the Hamiltonian (1.4). Final remark, the squeezing values are sensitive to the initial mean photon-numbers of the modes which can vanish completely for its large values.

B. Sub-Poissonian statistics

Sub-Poissonian light is an example of nonclassical light which can be measured by photodetectors. A state (of a single mode for convenience) which displays sub-Poisson statistics

is characterized by the fact that the variance of the photon number $\langle(\Delta\hat{n}_j(t))^2\rangle$ is less than the average photon number $\langle\hat{n}_j(t)\rangle = \langle\hat{A}_j^\dagger(t)\hat{A}_j(t)\rangle$. This can be expressed by means of the normalized normal second-order correlation function as

$$\begin{aligned} g_j^{(2)}(t) &= \frac{\langle\hat{A}_j^{\dagger 2}(t)\hat{A}_j^2(t)\rangle}{\langle\hat{A}_j^\dagger(t)\hat{A}_j(t)\rangle^2} \\ &= 1 + \frac{\langle(\Delta\hat{n}_j(t))^2\rangle - \langle\hat{A}_j^\dagger(t)\hat{A}_j(t)\rangle}{\langle\hat{A}_j^\dagger(t)\hat{A}_j(t)\rangle^2}, \end{aligned} \quad (3.6)$$

where the subscript j relates to the j th mode. Then it holds that $g_j^{(2)}(t) < 1$ for sub-Poissonian distribution, $g_j^{(2)}(t) > 1$ for super-Poissonian distribution and when $g_j^{(2)}(t) = 1$ Poisson distribution of coherent photons occurs. Also the system exhibits maximum sub-Poissonian statistics when $g_j^{(2)}(t) = 0$. Here we may mention that Fock state, chaotic field and coherent state are representing good examples for sub-Poissonian, super-Poissonian and Poissonian statistics, respectively. Moreover, the generation of sub-Poissonian light has been established in a semiconductor laser [34] and in the microwave region using masers operating in the microscopic regime [35] (for review see [36]).

On the other hand, it is worth referring to photon antibunching (bunching) phenomenon, which is generally not equivalent to sub-Poissonian (super-Poissonian) photon statistics [37, 38]. The basic formula to study this phenomenon is the two-time normalized intensity correlation function [38, 39], which can be represented as the joint detection probability of two photons, one at time t and another at time $t + \tau$, where τ is the time interval between the two-photon detection process. Nevertheless, the bunching/antibunching and super-/sub-Poissonian statistics are identical to the stationary fields. For more details about the connection between these two phenomena, different definitions as well as applications the reader can consult [39].

Now we investigate the sub-Poissonian statistics for our model when all modes are initially in the Fock states as we did for squeezing. In this case the moments $\langle\hat{A}_1^\dagger(t)\hat{A}_1(t)\rangle$ and $\langle\hat{A}_1^{\dagger 2}(t)\hat{A}_1^2(t)\rangle$ for the 1st mode read

$$\begin{aligned} \langle\hat{A}_1^\dagger(t)\hat{A}_1(t)\rangle &= [f_1^2(t) + f_2^2(t)]\bar{n}_1 + [f_3^2(t) + f_4^2(t)]\bar{n}_2 \\ &+ [f_5^2(t) + f_6^2(t)]\bar{n}_3 + f_2^2(t) + f_4^2(t) + f_6^2(t), \end{aligned} \quad (3.7a)$$

$$\begin{aligned} \langle\hat{A}_1^{\dagger 2}(t)\hat{A}_1^2(t)\rangle &= f_1^4(t)\bar{n}_1(\bar{n}_1 - 1) + f_2^4(t)(\bar{n}_1 + 1)(\bar{n}_1 + 2) + f_3^4(t)\bar{n}_2(\bar{n}_2 - 1) \\ &+ f_4^4(t)(\bar{n}_2 + 1)(\bar{n}_2 + 2) + f_5^4(t)\bar{n}_3(\bar{n}_3 - 1) + f_6^4(t)(\bar{n}_3 + 1)(\bar{n}_3 + 2) \end{aligned}$$

$$\begin{aligned}
& +f_5^2(t)f_6^2(t)(2\bar{n}_3+1)^2 + [f_1(t)f_2(t)(2\bar{n}_1+1) + f_3(t)f_4(t)(2\bar{n}_2+1)]^2 \\
& +4f_1^2(t)\bar{n}_1[f_3^2(t)\bar{n}_2 + f_4^2(t)(\bar{n}_2+1)] \\
& +4f_2^2(t)[f_3^2(t)\bar{n}_2(\bar{n}_1+1) + f_4^2(t)(\bar{n}_1+1)(\bar{n}_2+1)] \\
& +2(2\bar{n}_3+1)f_5(t)f_6(t)[f_1(t)f_2(t)(2\bar{n}_1+1) + f_3(t)f_4(t)(2\bar{n}_2+1)] \\
& +4[f_5^2(t)\bar{n}_3 + f_6^2(t)(\bar{n}_3+1)][f_1^2(t)\bar{n}_1 + f_2^2(t)(\bar{n}_1+1) + f_3^2(t)\bar{n}_2 + f_4^2(t)(\bar{n}_2+1)]; \quad (3.7b)
\end{aligned}$$

as we have mentioned earlier \bar{n}_j is the mean photon number of the j th mode. The expressions associated with the 2nd and 3rd modes can be obtained from (3.7) using the transformations (2.7).

Let us start our discussion when $\bar{n}_1 = \bar{n}_2 = \bar{n}_3 = \bar{n}$ and also consider the case of negligible contribution from parametric amplifier ($\lambda_1 \sim 0$). In this case the normalized normal second-order correlation function for the 1st mode reduces to

$$g_1^{(2)}(t) = 2 - (1 + \frac{1}{\bar{n}})[f_1^4(t) + f_3^4(t) + f_5^4(t)]. \quad (3.8)$$

From the identity (2.6) one can show that $0 < (f_1^4(t) + f_3^4(t) + f_5^4(t)) \leq 1$ and thus

$$2 > g_1^{(2)}(t) \geq (1 - \frac{1}{\bar{n}}), \quad (3.9)$$

which means that the model, in this case, can exhibit only sub-Poissonian statistics or partial coherence.

Now we can investigate the evolution of $g_j^{(2)}(t)$ when the modes are initially prepared in the number state $|1, 1, 1\rangle$ for the 1st and 3rd modes, as shown in Figs. 4a,b, respectively, for shown values. In Fig. 4a one can observe that $g_1^{(2)}(t)$ has smoothed behaviour (see, solid and long-dashed curves), i.e. it goes rapidly from values corresponding to the sub-Poissonian statistics to those for super-Poissonian ones and becomes almost stable for large interaction times. We further see that the stronger the interaction, the shorter the sub-Poissonian interval. Similar behaviour is available in a short interaction time if one turns his attention to $g_3^{(2)}(t)$, see Fig. 4b. However, in the large interaction times $g_3^{(2)}(t)$ becomes stable in a sense of periodic oscillations. So, generally, we can see that for the Hamiltonian model (1.4), the modes lose their sub-Poissonian character and provide partially coherent, chaotic and superchaotic statistics for large interaction time. We should comment here that the behaviour of the 3rd mode in this model is different from that of the usual squeezed number states given in the literature earlier [2] even if they can provide a similar behaviour for the quadrature squeezing. This fact is clear by comparing the behaviour of the second-order correlation function of the 3rd mode with that of the usual number states [28] where for the latter (with $\bar{n} \neq 0$) $g^{(2)}(0)$ has smoothed behaviour and satisfies the inequality

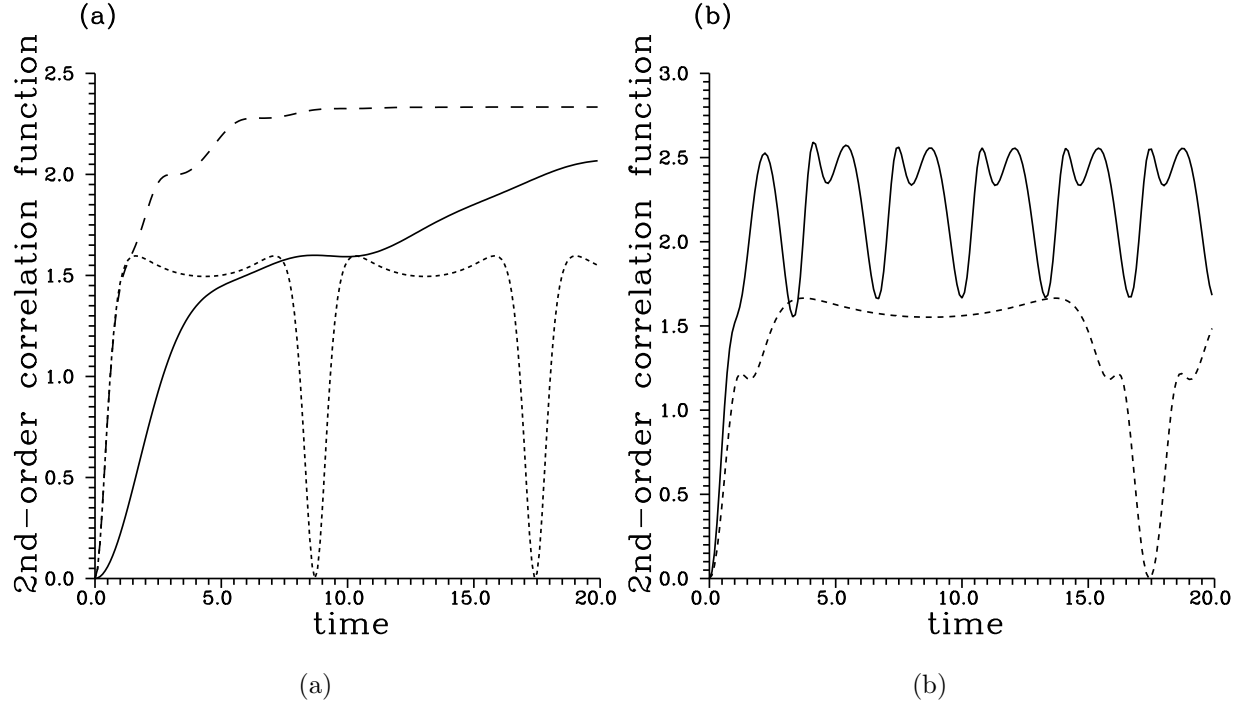


FIG. 4: Normalized normal second-order correlation function $g_j^{(2)}(t)$ against time for the modes which are initially in the number state $|1, 1, 1\rangle$ for a) the 1st mode for $(\lambda_1, \lambda_2, \lambda_3) = (0.6, 0.7, 0)$ (short-dashed curve), $(0.6, 0.7, 0.7)$ (long-dashed curve), and $(0.1, 0.2, 0.2)$ (solid curve); b) the 3rd mode for $(\lambda_1, \lambda_2, \lambda_3) = (0.6, 0.7, 0)$ (dashed curve), and $(0.6, 0.7, 0.7)$ (solid curve).

$0 \leq g^{(2)}(0) \leq 1.7$. On the other hand, if one compares the short-dashed curves with the solid ones in Figs. 4a,b, it is easy to recognize that the two-mechanism interaction system [11] ($\lambda_3 = 0$) conserves the initial sub-Poissonian statistics of the interacting modes which can be periodically recovered with period $t \simeq 8$ (for the 1st mode) and $t \simeq 16$ (for the 3rd mode). Also similar approach is available for the model including competition between two parametric amplifiers and one parametric frequency converter [30].

The second quantity we are planning to study here is the violation of Cauchy-Schwarz inequality. This quantity shows the anticorrelation effects in the compound modes and can be observed in a two-photon interference experiment [40]. This quantity can be represented by the factor [41]

$$I_{j,k}(t) = \frac{[\langle \hat{A}_j^{\dagger 2}(t) \hat{A}_j^2(t) \rangle \langle \hat{A}_k^{\dagger 2}(t) \hat{A}_k^2(t) \rangle]^{\frac{1}{2}}}{\langle \hat{A}_j^{\dagger}(t) \hat{A}_j(t) \hat{A}_k^{\dagger}(t) \hat{A}_k(t) \rangle} - 1. \quad (3.10)$$

The negative values for the quantity $I_{j,k}(t)$ mean that the intermodal correlation is larger than the correlation between photons in the same mode [42] and this indicates strong vio-

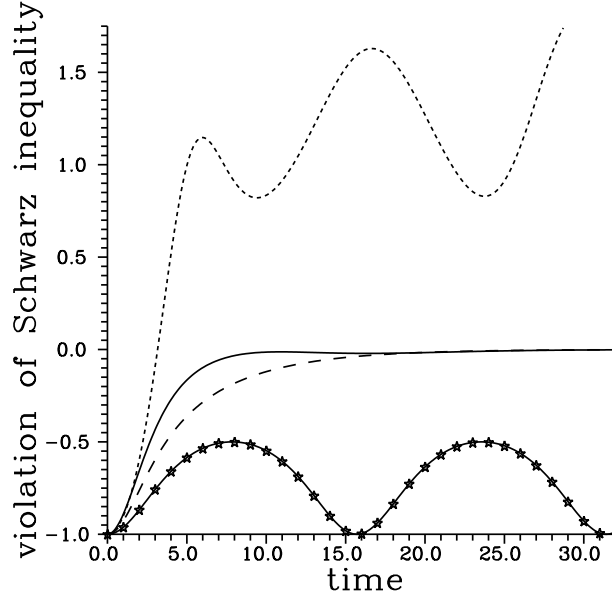


FIG. 5: Evolution of the quantity $I_{j,k}(t)$ against the time for $(\bar{n}_j, \lambda_j) = (1, 0.1), j = 1, 2, 3$. The solid and short-dashed curves represent the above quantity obtained in (1,2) and (1,3) modes, respectively. The long-dashed and star-centered curves are given for $(\lambda_1, \lambda_2, \lambda_3) = (0.1, 0, 0)$ and $(0, 0.1, 0)$, respectively, with $\bar{n}_j = 1$.

lation of the Cauchy-Schwarz inequality.

The resulting expression for $\langle \hat{A}_j^\dagger(t) \hat{A}_j(t) \hat{A}_k^\dagger(t) \hat{A}_k(t) \rangle$ is lengthy and will not be reproduced here. In Fig. 5 we have plotted the quantity $I_{j,k}(t)$ indicating the violation of Cauchy-Schwarz inequality between the j th mode and the k th mode in dependence on time where $(\bar{n}_j, \lambda_j) = (1, 0.1), j = 1, 2, 3$. Further, the solid and short-dashed curves represent the quantity (3.10) obtained in (1,2) and (1,3) modes, respectively. For the sake of comparison the long-dashed curve is given for the single parametric amplifier, i.e. $(\lambda_1, \lambda_2, \lambda_3) = (0.1, 0, 0)$, for the same values of \bar{n}_j . Similarly the star-centered curve is given for the single frequency converter. In this figure the characters of both the Fock states and the structure of the Hamiltonian, (1.4), are reflected in the behaviour of the curves. To be more specific, the nonclassical negative values are dominant after switching on of the interaction. Also the behaviour of the $I_{1,2}(t)$ is smooth and becomes stable for large values of interaction times, however, that of the $I_{1,3}(t)$ undergoes amplification as well as oscillatory behaviour as a result of the energy exchange between these two modes in the system (cf. (1.4)). On the other hand, the comparison of the solid and long-dashed curves shows that the behaviour of

the $I_{1,2}(t)$ is close to that of the single parametric amplifier and for both $I_{1,2}(t) \leq 0$ for all times. This is in contrast with the behaviour of the two processes for the sum-squeezing, see Fig. 3. Nevertheless, this is not the case for the short-dashed (i.e. $I_{1,3}(t)$) and star-centered curves where the former can exhibit anticorrelation only for a short time after switching on of the interaction, however, the latter evolves periodically with period $t = 2\pi/\lambda_2$ displaying always anticorrelation between modes. Further, similar behaviour can be seen regardless of the values of λ_j . Finally, the behaviour of the $I_{2,3}(t)$ is similar to that of the $I_{1,3}(t)$.

IV. QUASIPROBABILITY FUNCTIONS

There are three types of quasiprobability functions: Wigner W -, Glauber P -, and Husimi Q -functions. These functions can be used as crucial to describe the nonclassical effects of the system, e.g. one can employ negative values of W -function, stretching of Q -function and high singularities in P -function. Also, these functions are now accessible from measurements [43].

Indeed, the detailed statistics of the three coupled field modes can be obtained from photon-counting experiments. Most often we are interested in the quantum statistics of either one mode which determine the ensemble averages of the observables of this mode, or the composite statistics of the compound modes which reflect their mutually correlated properties, so that in the following we consider phase space distributions, in particular, W -function for the single- and compound-modes when all modes are initially prepared in number states. To achieve this goal we calculate the s -parametrized joint characteristic function defined by

$$C^{(3)}(\underline{\zeta}, t, s) = \text{Tr} \left\{ \hat{\rho}(0) \exp \left[\sum_{j=1}^3 (\zeta_j \hat{A}_j^\dagger(t) - \zeta_j^* \hat{A}_j(t) + \frac{s}{2} |\zeta_j|^2) \right] \right\}, \quad (4.1)$$

where $\hat{\rho}(0)$ is the initial density matrix operator for the system under consideration, $\underline{\zeta} = (\zeta_1, \zeta_2, \zeta_3)$, and s takes on values 1, 0 and -1 corresponding to normally, symmetrically and antinormally ordered characteristic functions, respectively. The superscript 3 stands for three-mode case. When the modes are initially in number states $|n_1, n_2, n_3\rangle$; the symmetrical characteristic function can be calculated in a straightforward way as

$$C^{(3)}(\underline{\zeta}, s = 0, t) = \prod_{j=1}^3 \exp\left(-\frac{1}{2} |\eta_j(t)|^2\right) L_{n_j}(|\eta_j(t)|^2), \quad (4.2)$$

where L_n is the Laguerre polynomial of order n and $\eta_j(t)$ are given by

$$\eta_1(t) = \zeta_1 f_1(t) - \zeta_1^* f_2(t) - \zeta_2 g_3(t) + \zeta_2^* g_4(t) + \zeta_3 h_5(t) - \zeta_3^* h_6(t), \quad (4.3a)$$

$$\eta_2(t) = \zeta_2 g_1(t) - \zeta_2^* g_2(t) - \zeta_1 f_3(t) + \zeta_1^* f_4(t) + \zeta_3 h_3(t) - \zeta_3^* h_4(t), \quad (4.3b)$$

$$\eta_1(t) = \zeta_3 h_1(t) - \zeta_3^* h_2(t) + \zeta_1^* f_6(t) - \zeta_1 f_5(t) - \zeta_2 g_5(t) + \zeta_2^* g_6(t). \quad (4.3c)$$

We proceed by giving the definition of the s -parametrized joint quasiprobability functions as

$$W^{(3)}(\underline{\alpha}, t, s) = \frac{1}{\pi^6} \int \int \int C^{(3)}(\underline{\zeta}, t, s) \prod_{j=1}^3 \exp(\alpha_j \zeta_j^* - \alpha_j^* \zeta_j) d^2 \zeta_j, \quad (4.4)$$

where $\underline{\alpha} = (\alpha_1, \alpha_2, \alpha_3)$. When $s = 1, 0, -1$, the formula (4.4) gives formally Glauber P -function, Wigner W -function and Husimi Q -function, respectively. Now substituting from (4.2) into (4.4) and performing the integration we get the joint Wigner function as

$$W^{(3)}(\underline{\alpha}, t) = \frac{8(-1)^{n_1+n_2+n_3}}{\pi^3} \prod_{j=1}^3 \exp(-2|\epsilon_j(t)|^2) L_{n_j}(4|\epsilon_j(t)|^2), \quad (4.5)$$

where $\epsilon_j(t)$ are

$$\epsilon_1(t) = \alpha_1 f_1(t) - \alpha_1^* f_2(t) - \alpha_2 g_3(t) + \alpha_2^* g_4(t) + \alpha_3 h_5(t) - \alpha_3^* h_6(t), \quad (4.6a)$$

$$\epsilon_2(t) = \alpha_1^* f_4(t) - \alpha_1 f_3(t) + \alpha_2 g_1(t) - \alpha_2^* g_2(t) + \alpha_3 h_3(t) - \alpha_3^* h_4(t), \quad (4.6b)$$

$$\epsilon_3(t) = \alpha_1^* f_6(t) - \alpha_1 f_5(t) + \alpha_2^* g_6(t) - \alpha_2 g_5(t) + \alpha_3 h_1(t) - \alpha_3^* h_2(t). \quad (4.6c)$$

It is evident from (4.5) that the joint functions are strongly affected by the correlation between modes; this is reflected in the cross terms between different amplitudes of different modes. Such correlations have been used in a number of studies on nonclassical aspects of light including questions of violation of Bell inequalities [44].

On the other hand, the W -function of the single-mode can be obtained by means of integrating two times in the the joint W -function (4.5) or by using the following relation

$$W^{(1)}(\alpha, t) = \frac{1}{\pi^2} \int \int C^{(1)}(\zeta_j, t) \exp(\alpha \zeta_j^* - \alpha^* \zeta_j) d^2 \zeta_j, \quad (4.7)$$

where $C^{(1)}(\zeta_j, t)$ is the single-mode symmetrical characteristic function which can be obtained from the joint symmetrical characteristic function (4.2). For instance, the characteristic function for mode \hat{A}_1 (say) can be obtained from (4.2) by simply setting $\zeta_2 = \zeta_3 = 0$. Now the single-mode Wigner function for the 1st mode when it is in the Fock states $|n_1\rangle$ and the rest modes are in vacuum can be obtained from (4.7) together with (4.2) (after putting $\zeta_2 = \zeta_3 = 0$ in (4.2)), carrying out the integration, as

$$W^{(1)}(\alpha, t) = \frac{2(-1)^{n_1}}{\pi \sqrt{A_-(t)A_+(t)}} \exp \left[\frac{2h_+(t)}{A_-(t)A_+(t)} \right] \sum_{l=0}^{n_1} \left[\frac{B_-(t)}{A_-(t)} \right]^{(n_1-l)} \left[\frac{B_+(t)}{A_+(t)} \right]^l \\ \times L_{n_1-l}^{-\frac{1}{2}}(z_1(t)) L_l^{-\frac{1}{2}}(z_2(t)), \quad (4.8)$$

where

$$A_{\pm}(t) = [f_1(t) \pm f_2(t)]^2 + [f_3(t) \pm f_4(t)]^2 + [f_5(t) \pm f_6(t)]^2,$$

$$B_{\pm}(t) = [f_1(t) \pm f_2(t)]^2 - [f_3(t) \pm f_4(t)]^2 - [f_5(t) \pm f_6(t)]^2,$$

$$C_{\pm}(t) = (\alpha^2 + \alpha^{*2})[f_1(t)f_2(t) \pm f_3(t)f_4(t) \pm f_5(t)f_6(t)],$$

$$D_{\pm}(t) = -|\alpha|^2[f_1^2(t) + f_2^2(t) \pm f_3^2(t) \pm f_4^2(t) \pm f_5^2(t) \pm f_6^2(t)],$$

$$h_{\pm}(t) = C_{\pm}(t) + D_{\pm}(t),$$

$$\begin{aligned} z_1(t) &= \frac{2[A_-(t) + B_-(t)][A_-(t)h_-(t) - B_-(t)h_+(t)]}{A_-(t)B_-(t)[A_+(t)B_-(t) - A_-(t)B_+(t)]}, \\ z_2(t) &= \frac{2[A_+(t) + B_+(t)][B_+(t)h_+(t) - A_+(t)h_-(t)]}{A_+(t)B_+(t)[A_+(t)B_-(t) - A_-(t)B_+(t)]}. \end{aligned} \quad (4.9)$$

The expressions for the 2nd and 3rd modes can be obtained from (4.8) using the transformations (2.7).

One can easily check when $t \rightarrow 0$ that the expression (4.8) reduces to the well-known W -function of Fock state $|n_1\rangle$. In this case the following identity [45]

$$\sum_{l=0}^{n_1} L_l^{\nu_1}(x) L_{n_1-l}^{\nu_2}(y) = L_{n_1}^{\nu_1+\nu_2+1}(x+y) \quad (4.10)$$

has to be used.

Now we proceed by studying the evolution of the W -function for the 1st mode when it is initially in the Fock state $|1\rangle$ and the other modes are in vacuum using the expression (4.8). In fact, the W -function of the Fock state $|1\rangle$ is well known and it exhibits an inverted hole with more pronounced negative values related to the state showing maximum sub-Poissonian statistics. However, this behaviour can be completely washed out in our model at certain values of interaction parameters. This can be seen in Fig. 6a where one can observe the well-known shape for the W -function of the thermal light, which is broader than that for vacuum and this demonstrates the Bose-Einstein statistics for thermal light exhibiting larger fluctuations than for coherent light. So the competition between different states in the model (power transfers) can cause that the output field exhibits classical nature of thermal light. In Fig. 6b, by increasing the values of the coupling constants, W -function for squeezed thermal light dominates. This result is different from that given in section 3 since there the

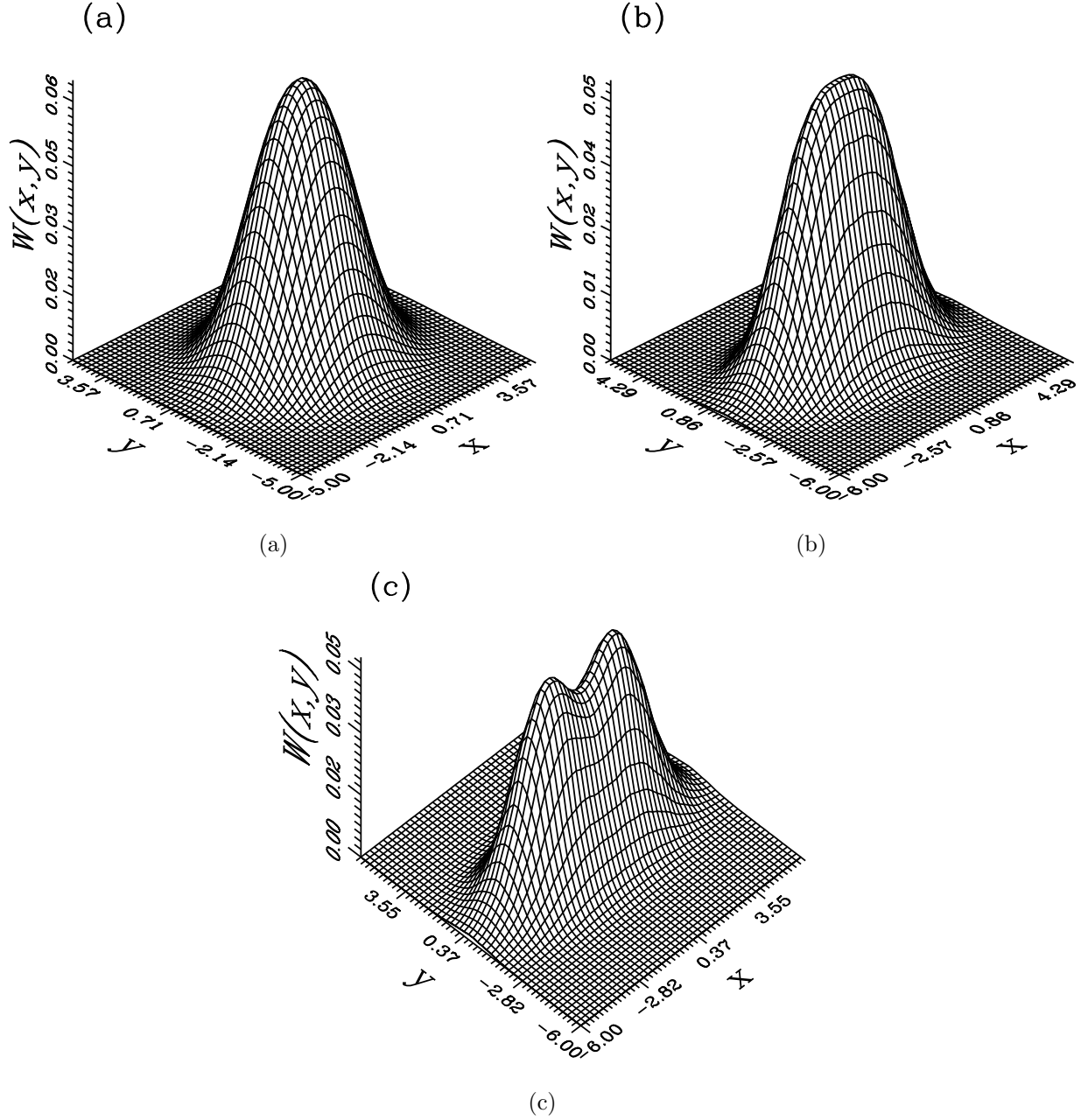


FIG. 6: W -function against x and y for the 1st mode when it is in the Fock state $|1\rangle$ and the other modes are in vacuum for a) $(t, \lambda_1, \lambda_2, \lambda_3) = (\frac{\pi}{2}, 1.005, 1, 0.1)$; b) $(t, \lambda_1, \lambda_2, \lambda_3) = (\frac{\pi}{2}, 1.008, 1, 0.4)$; c) $(t, \lambda_1, \lambda_2, \lambda_3) = (\pi, 0.5, 0.4, 0.4)$.

initial thermal fields undergo squeezing when evolve in the present structure. It is important to mention that stretching here can be more pronounced for large interaction time. Finally, Fig. 6c displays an interesting fact that a statistical mixture for coherent superposition states, in principle, can also be realized where the basis of the two Gaussian bells dominates in the behaviour of W -function. This behaviour may be achieved also from the cat states

when they interact with a finite temperature heat bath [46] or with the bath which consists of a gain medium in addition to the usual absorber [47]. For example, in the latter case this can be realized by choosing the gain appropriately so that one gets a purely diffusive motion of the field mode which leads to a double Gaussian structure with the missing oscillatory behaviour. Thus based on the fact that the nonlinear coupling between modes is present in the medium, the fields which are initially nonclassical cannot recover their properties during the evolution in the model for strong coupling and large interaction time. Nevertheless, they lose some nonclassical features, e.g. the W -function loses its negative values, and is obtaining other ones, e.g. stretching of its form.

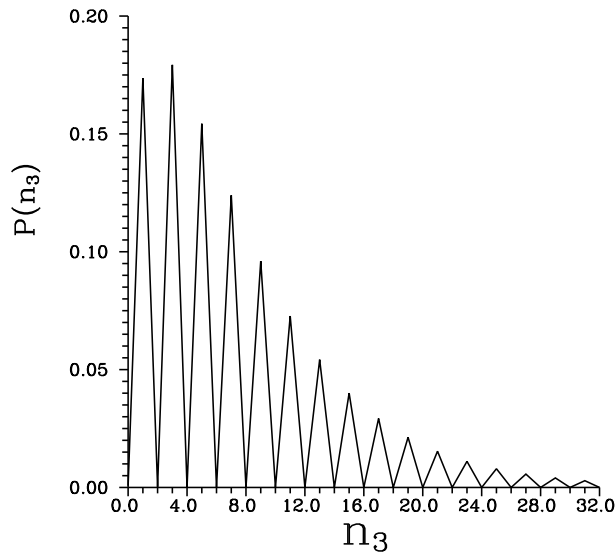


FIG. 7: photon-number distribution $P(n_3)$ for the 3rd mode when it is initially in the Fock state $|1\rangle$ and the other modes are in vacuum for $t = 8$ and $(\lambda_1, \lambda_2, \lambda_3) = (0.3, 0.3, 0.3)$.

Finally, we would like to close this section by paying attention to the behaviour of the photon-number distribution when the modes are initially in Fock states. This will be done by means of the integral expression for the photon-number distribution in terms of Wigner function and Laguerre polynomials, which is given by

$$P(n_j) = \frac{2(-1)^{n_j}}{n_j!} \int W^{(1)}(\alpha) \exp(-2|\alpha|^2) L_{n_j}(4|\alpha|^2) d^2\alpha, \quad (4.11)$$

where j denotes the mode under consideration and $W^{(1)}(\alpha)$ is the single-mode Wigner function. We restrict ourselves to the photon-number distribution for the 3rd mode when it is initially in Fock state $|1\rangle$ and the other modes are in vacuum. After inserting the expression for W -function of this case into (4.11) and performing the integral, the result has

been plotted in Fig. 7 for shown values. In this figure one can see the oscillatory behaviour typical for the photon-number distribution of squeezed states in the 3rd mode. This is clear in the pairwise nature of the oscillations, i.e. $P(2n_3) = 0$, n_3 is positive integer. Indeed, for the squeezed states, i.e. squeezed vacuum, squeezed number and squeezed thermal states, these pairwise oscillations are explained as the result of the quadratic, or two-photon nature of the squeeze operator $\hat{S}(r)$ [2].

V. CONCLUSION

In this article we have studied the statistical properties of three harmonic oscillators mutually interacting in the nonlinear crystal. The model is governed by interaction Hamiltonian including competition between two frequency converters and one parametric amplifier. After using the Heisenberg approach to the quantum statistics of interacting modes, we have investigated effects produced by the dynamics of the interaction as well as by the nonclassical behaviour of the initial light modes. In our analysis we have considered that the modes are initially in the number states. We have proved that squeezed light can be generated in the standard sense or in the correlated quadratures (sum-squeezing). Furthermore, we have shown that this is still valid if the Fock states are replaced by thermalized fields. In this case the model operates as a microwave Josephson-junction parametric amplifier. We have also demonstrated that the initial sub-Poissonian statistics of the interacting modes are washed out, which leads to partially coherent, chaotic and superchaotic fields. Finally, we have shown that when the system is initially prepared in the Fock state $|1, 0, 0\rangle$, at certain values of interaction parameters, the 1st mode can evolve into thermal states or in squeezed thermal states.

Acknowledgments

We thank Prof. V. Peřinová and Dr. A. Lukš from Department of Optics, Palacký University, Olomouc, Czech Republic for the critical reading of the article. J. P. and F. A. A. E-O. acknowledge the partial support from the Projects LN00A015 and Research Project CEZ: J 14/98 of Czech Ministry of Education and 202/00/0142 of Czech grant agency. One of us (M. S. A.) is grateful for the financial support from the Project Math 1418/19 of the

Research Centre, College of Science, King Saud University.

- [1] B. R. Mollow and R. J. Glauber, Phys. Rev. **160**, 1076 (1967); *ibid.* 1097.
- [2] H. P. Yuen, Phys. Rev. A **13**, 2226 (1976).
- [3] J. Peřina, *Quantum Statistics of Linear and Nonlinear Optical Phenomena*, 2nd ed. (Kluwer, Dordrecht, 1991).
- [4] W. J. Mielniczuk and J. Chrostowski, Phys. Rev. A **23**, 1382 (1981).
- [5] Y. N. Orlov and V. V. Vedenyapin, Mod. Phys. Lett. **9**, 291 (1993).
- [6] W. Louisell, *Radiation and Noise in Quantum Electronics* (McGraw-Hill, New York, 1964), p. 274.
- [7] J. Janszky, C. Sibilía and M. Bertolotti, J. Mod. Opt. **38**, 2467 (1991); V. Peřinová, A. Lukš, J. Křepelka, C. Sibilía and M. Bertolotti, J. Mod. Opt. **38**, 2429 (1991); J. Herec, Acta Phys. Slov. **49**, 731 (1999); L. Miřta, Acta Phys. Slov. **49**, 737 (1999).
- [8] D. Marcuse, *Theory of Optical Dielectric Waveguides* (New York: Academic Press 1974), p. 1.
- [9] W. H. Louisell, A. Yariv and A. E. Siegman, Phys. Rev. A **124**, 1646 (1961).
- [10] G. A. Garrett, A. G. Rojo, A. K. Sood, J. F. Whitaker and R. Merlin, Science **275**, 1638 (1997).
- [11] E. A. Mishkin and D. F. Walls, Phys. Rev. **185**, 1618 (1969).
- [12] M. E. Smithers and E. Y. C. Lu, Phys. Rev. A **10**, 1874 (1974).
- [13] J. Janszky, C. Sibilía and M. Bertolotti, P. Adam and A. Petak, Quant. Semiclass. Opt. **7**, 509 (1995).
- [14] M. S. Abdalla, F. A. A. El-Orany and J. Peřina, Phys. A: Math. Gen. **32**, 3457 (1999).
- [15] L. E. Myers, R. C. Eckardt, M. M. Fejer, R. L. Byer, W. R. Bosenberg and J. W. Pierce, J. Opt. Soc. Am. B **12**, 2102 (1995); L. E. Myers, R. C. Eckardt, M. M. Fejer, R. L. Byer and W. R. Bosenberg, Opt. Lett. **21**, 591 (1996); A. P. Alodjants, S. M. Arakelian and A. S. Chirkin, Quant. Semiclass. Opt. **9**, 311 (1997).
- [16] S. M. Barnett and P. L. Knight, J. Opt. Soc. Am. B **2**, 467 (1985); S. M. Barnett and P. L. Knight, J. Mod. Opt. **34**, 841 (1987); L. Gilles and P. L. Knight, J. Mod. Opt. **39**, 1411 (1992).

- [17] Y. Yamamoto and H. A. Haus, *Rev. Mod. Phys.* **58**, 1001 (1986).
- [18] M. C. Teich, F. Capasso and B. E. Saleh, *J. Opt. Soc. Am. B* **4**, 1663 (1987).
- [19] A. Heidmann, R. J. Horowicz, S. Reynaoud, E. Giacobino, C. Fabre and C. Camy, *Phys. Rev. Lett.* **59**, 2555 (1987).
- [20] B. T. H. Varcoe, S. Brattke and H. Walther, *Quant. Semiclass. Opt.* **2**, 154 (2000).
- [21] See Special Issue on *Squeezed Light*, *J. Mod. Opt.* **34**, (1987), edited by R. Loudon and P. L. Knight; also *Nonclassical Effects in Quantum Optics* (AIP, New York 1991), edited by P. Meystre and D. F. Walls.
- [22] C. M. Caves, *Phys. Rev. D* **23**, 1693 (1981).
- [23] H. P. Yuen and J. H. Shapiro, *Opt. Lett.* **4**, 334 (1979); D. F. Walls and P. Zoller, *Phys. Rev. Lett.* **47**, 709 (1981); G. J. Milburn and D. F. Walls, *Opt. Commun.* **39**, 401 (1981); L. A. Lugiato and G. Strini, *Opt. Commun.* **41**, 67 (1982); *ibid.* **41**, 447 (1982).
- [24] M. Hillery, *Phys. Rev. A* **40**, 3147 (1989).
- [25] L. Mandel, *Opt. Commun.* **42**, 437 (1982).
- [26] B. Yurke, *J. Opt. Soc. Am. B* **4**, 1551 (1987).
- [27] P. Marian and T. A. Marian, *Phys. Rev. A* **47**, 4474 (1993).
- [28] M. S. Kim, F. A. M. de Oliveria and P. L. Knight, *Phys. Rev. A* **40**, 2494 (1989); M. S. Kim, F. A. M. de Oliveira and P. L. Knight, *Opt. Commun.* **72**, 99 (1989); P. Marian, *Phys. Rev. A* **44**, 3325 (1991); P. Marian, *Phys. Rev. A* **45**, 2044 (1992).
- [29] H. Fearn and M. J. Collet, *J. Mod. Opt.* **35**, 553 (1988).
- [30] M. S. Abdalla, M. M. A. Ahmed and S. Al-Homidan, *J. Phys. A: Math. Gen.* **31**, 3117 (1998).
- [31] M. Hillery, *Phys. Rev. A* **36**, 3796 (1987); *ibid.* *Opt. Commun.* **62**, 135 (1987).
- [32] B. Yurke, S. McCall and J. Klauder, *Phys. Rev. A* **33**, 4033 (1986).
- [33] M. Hillery, D. Yu and J. Bergou, *Workshop on Squeezed States and Uncertainty Relations*, (NASA, Maryland, 1992), p.125.
- [34] Y. Yamamoto and S. Machida, *Phys. Rev. A* **35**, 5114 (1987).
- [35] G. Rempe, F. Schmidt-Kaler and H. Walther, *Phys. Rev. Lett.* **64**, 2783 (1990).
- [36] M. C. Teich and B. E. Saleh, in *Progress in Optics*, Vol. 26, edited by E. Wolf (North-Holland, Amsterdam 1988).
- [37] S. Singh, *Opt. Comm.* **44**, 254 (1983).
- [38] X. T. Zou and L. Mandel, *Phys. Rev. A* **41**, 475 (1990).

- [39] A. Miranowicz, J. Bajer, A. Ekert and W. Leoński, *Acta Physica Slovaca* **47**, 319 (1997); A. Miranowicz, J. Bajer, H. Matsueda, M. R. B. Wahiddin and R. Tanaś R, *Quant. Semiclass. Opt.* **1**, 511 (1999); *ibid.* *Quant. Semiclass. Opt.* **1**, 603 (1999).
- [40] L. Mandel, *Phys. Rev. A* **28**, 929 (1983); R. Ghosh and L. Mandel, *Phys. Rev. Lett.* **59**, 1903 (1987).
- [41] G. S. Agarwal, *J. Opt. Soc. Am. B* **5**, 1940 (1988).
- [42] L. Gilles and P. L. Knight, *J. Mod. Opt.* **39**, 1411 (1992).
- [43] U. Leonhardt, *Measuring the Quantum State of Light* (University Press, Cambridge 1997).
- [44] G. S. Agarwal, *Quant. Opt.* **2**, 1 (1990).
- [45] I. S. G. Gradshteyn and I. M. Ryzhik: *Table of Integrals, Series, and Products* (Academic, Boston 1994).
- [46] M. S. Kim and V. Bužek, *Phys. Rev. A* **46**, 4239 (1992).
- [47] G. S. Agarwal, *Phys. Rev. A* **59**, 3071 (1999).